

UNITARITY SCREENINGS IN HIGH ENERGY SCATTERING

Uri Maor

Raymond and Beverly Sackler Faculty of Exact Science

Tel Aviv University, Tel Aviv, 69978, Israel

DEDICATED TO THE MEMORY OF ALIOSHA KAIDALOV

INTRODUCTION

Unitarity screening considerations, below saturation, date back to the ISR epoch, where they provided a simple bypass over seeming paradoxes.

1) Whereas non screened σ_{tot} grows like a power s^Δ , σ_{el} grows faster, like $s^{2\Delta}$ (up to $\log(s)$ corrections). With no screening, σ_{el} will, eventually, be larger than σ_{tot} .

2) Even though elastic and diffractive scatterings are dynamically similar, the energy dependence of diffractive cross sections is significantly more moderate.

3) The elastic amplitude is central in impact parameter b , peaking at $b=0$.

The diffractive amplitudes are peripheral, peaking at large b , which gets larger with energy.

Estimates of high energy soft scatterings require a unified analysis of elastic and diffractive scatterings, incorporating s and t unitarity screenings.

S-CHANNEL UNITARITY

The simplest s-channel unitarity bound on $a_{el}(s, b)$ is obtained from a diagonal re-scattering matrix, where repeated elastic re-scatterings secure s-channel unitarity, $2Ima_{el}(s, b) = |a_{el}(s, b)|^2 + G^{in}(s, b)$. i.e. At a given (s,b), $\sigma_{tot} = \sigma_{el} + \sigma_{inel}$. Its general solution is:

$$a_{el}(s, b) = i \left(1 - e^{-\Omega(s,b)/2}\right), \quad G^{in}(s, b) = 1 - e^{-\Omega(s,b)}. \quad \Omega \text{ is arbitrary.}$$

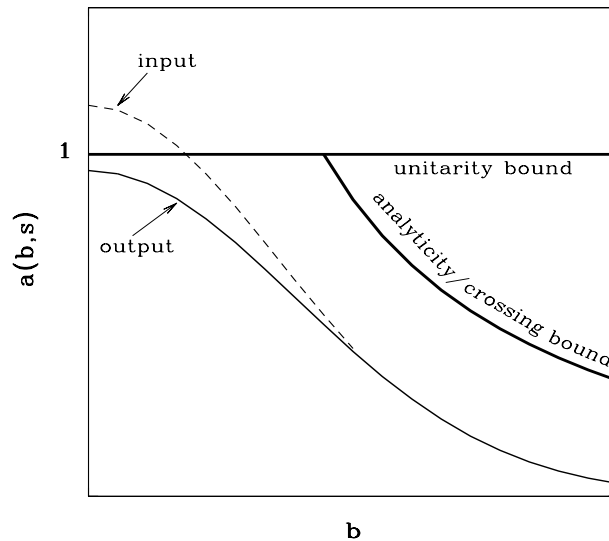
The output s-unitarity bound is $|a_{el}(s, b)| \leq 2$, leading to very large total and elastic LHC cross sections, which are not supported by TOTEM recent data.

In a Glauber type eikonal approximation, the input opacity $\Omega(s, b)$ is real. It equals to the imaginary part of the input Born term, a IP exchange in our context. The output $a_{el}(s, b)$ is imaginary.

The consequent bound is $|a_{el}(s, b)| \leq 1$, which is the black disc bound.

In a single channel eikonal model, the screened cross sections are:

$$\sigma_{tot} = 2 \int d^2b \left(1 - e^{-\Omega(s,b)/2}\right), \quad \sigma_{el} = \int d^2b \left(1 - e^{-\Omega(s,b)/2}\right)^2, \quad \sigma_{inel} = \int d^2b \left(1 - e^{-\Omega(s,b)}\right).$$



The figure shows the s-channel black bound of unity, and the bound implied by analyticity/crossing symmetry on the expanding b-amplitude. **The consequent Froissart-Martin bound is:** $\sigma_{tot} \leq C \ln^2(s/s_0)$, $s_0 = 1\text{GeV}^2$, $C \propto 1/2m_\pi^2 \simeq 30\text{mb}$.

C is far too large to be relevant at the TeV-scale.

s-unitarity implies: $\sigma_{el} \leq \frac{1}{2}\sigma_{tot}$ and $\sigma_{inel} \geq \frac{1}{2}\sigma_{tot}$. **At saturation,** $\sigma_{el} = \sigma_{inel} = \frac{1}{2}\sigma_{tot}$.

Introducing diffraction, significantly changes the features of s-unitarity.

However, the saturation signatures remain valid.

GOOD-WALKER DECOMPOSITION

Consider a system of two orthonormal states, a hadron Ψ_h and a diffractive state Ψ_D . Ψ_D replaces the continuous diffractive Fock states. Good-Walker (GW) noted that Ψ_h and Ψ_D do not diagonalize the 2x2 interaction matrix \mathbf{T} . Let Ψ_1 and Ψ_2 be eigen states of \mathbf{T} .

$$\Psi_h = \alpha\Psi_1 + \beta\Psi_2, \quad \Psi_D = -\beta\Psi_1 + \alpha\Psi_2, \quad \alpha^2 + \beta^2 = 1.$$

The eigen states initiate 4 $A_{i,k}$ elastic GW amplitudes ($\psi_i + \psi_k \rightarrow \psi_i + \psi_k$). $i,k=1,2$. For initial $p(\vec{p}) - p$ we have $A_{1,2} = A_{2,1}$. I shall follow the GLM definition, in which the mass distribution of Ψ_D is not defined and requires a specification. The elastic, SD and DD amplitudes in a 2 channel screened GW model are:

$$\begin{aligned} a_{el}(s, b) &= i\{\alpha^4 A_{1,1} + 2\alpha^2\beta^2 A_{1,2} + \beta^4 A_{2,2}\}, \\ a_{sd}(s, b) &= i\alpha\beta\{-\alpha^2 A_{1,1} + (\alpha^2 - \beta^2)A_{1,2} + \beta^2 A_{2,2}\}, \\ a_{dd}(s, b) &= i\alpha^2\beta^2\{A_{1,1} - 2A_{1,2} + A_{2,2}\}, \\ A_{i,k}(s, b) &= \left(1 - e^{\frac{1}{2}\Omega_{i,k}(s,b)}\right) \leq 1. \end{aligned}$$

GW mechanism changes the structure of unitarity below saturation.

- In the GW sector we obtain the Pumplin bound: $\sigma_{el} + \sigma_{diff}^{GW} \leq \frac{1}{2}\sigma_{tot}$.

σ_{diff}^{GW} is the sum of the GW soft diffractive cross sections.

- Below saturation, $\sigma_{el} \leq \frac{1}{2}\sigma_{tot} - \sigma_{diff}^{GW}$ and $\sigma_{inel} \geq \frac{1}{2}\sigma_{tot} + \sigma_{diff}^{GW}$.

- $a_{el}(s, b) = 1$, when and only when, $A_{1,1}(s, b) = A_{1,2}(s, b) = A_{2,2}(s, b) = 1$.

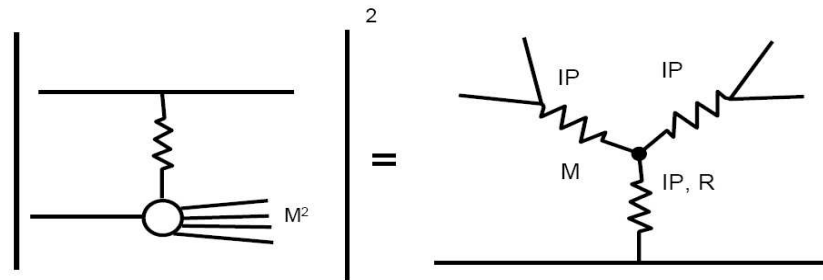
- When $a_{el}(s, b) = 1$, all diffractive amplitudes at the same (s,b) vanish.

- As we shall see, there is a distinction between GW and non GW diffraction.

Regardless, GW saturation signatures are valid also in the non GW sector.

- The saturation signature, $\sigma_{el} = \sigma_{inel} = \frac{1}{2}\sigma_{tot}$, in a multi channel calculation is coupled to $\sigma_{diff} = 0$. Consequently, prior to saturation the diffractive cross sections stop growing and start to decrease with energy.

This is a clear signature preceding saturation.



CROSSED CHANNELED UNITARITY

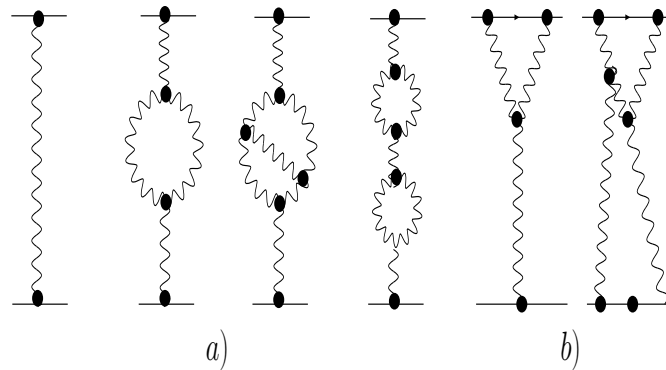
Translating the concepts presented into a viable phenomenology requires a specification of $\Omega(s, b)$, for which Regge Pomeron (IP) theory is a powerful tool.

Mueller(1971) applied 3 body unitarity to equate the cross section of

$a + b \rightarrow M_{sd}^2 + b$ to the triple Regge diagram $a + b + \bar{b} \rightarrow a + b + \bar{b}$, with a leading $3IP$ vertex term.

The $3IP$ approximation is valid when $\frac{m_p^2}{M_{sd}^2} \ll 1$ and $\frac{M_{sd}^2}{s} \ll 1$.

The leading energy/mass dependences are $\frac{d\sigma^{3IP}}{dt dM_{sd}^2} \propto s^{2\Delta_{IP}} \left(\frac{1}{M_{sd}^2}\right)^{1+\Delta_{IP}}$.



Mueller's $3IP$ approximation for non GW diffraction is the lowest order of t-channel multi IP interactions, compatible with t-channel unitarity.

Recall that unitarity screening of GW ("low mass") diffraction is carried out explicitly by eikonalization, while the screening of non GW ("high mass") diffraction is carried out by the survival probability (to be discussed).

The figure shows the IP Green function. Multi IP interactions are summed differently in the various IP models. Note the analogy with QED:

- a) Enhanced diagrams, present the renormalization of the propagator.
- b) Semi enhanced diagrams, present the pIP vertex renormalization.

SURVIVAL PROBABILITY

The experimental signature of a \mathbb{P} exchanged reaction is a large rapidity gap (LRG), devoid of hadrons in the $\eta - \phi$ Lego plot, $\eta = -\ln(\tan\frac{\theta}{2})$.

S^2 , the LRG survival probability, is a unitarity induced suppression factor of non GW diffraction, soft or hard: $S^2 = \sigma_{diff}^{screened} / \sigma_{diff}^{nonscreened}$.

It is the probability that the LRG signature will not be filled by debris (partons and/or hadrons) originating from either the s-channel re-scatterings of the spectator partons, or by the t-channel multi \mathbb{P} interactions.

Denote the gap survival factor initiated by s-channel eikonalization S_{eik}^2 , and the one initiated by t-channel multi \mathbb{P} interactions, $S_{m\mathbb{P}}^2$.

The incoming projectiles are summed over (i,k).

S^2 is obtained from a convolution of S_{eik}^2 and $S_{m\mathbb{P}}^2$.

A simpler, reasonable approximation, is $S^2 = S_{eik}^2 \cdot S_{m\mathbb{P}}^2$.

THE COMPONENTS OF DIFFRACTION

Many of my discussions with Aliosha ended with a civilized disagreement on the incorporation of the GW mechanism, with Mueller's approach.

Commonly, low mass diffraction is associated with GW and high mass diffraction is non GW, with a low 4-5 GeV bound.

Aliosha strongly believed (without a proof) that GW mass upper bound and Mueller's high mass lower bound coincide.

i.e. there is no overlap of low and high mass diffraction.

This point of view is shared by KMR, Ostapchenko and Poghosyan.

GLM offer (also without a proof) that GW and high mass diffraction have the same upper bound.

In GLM most of the diffraction is GW, while in KMR it is high mass.

GLM do not offer a diffractive mass distribution, which needs a dynamic specification.

THE PARTONIC POMERON

Current \mathbb{P} models differ in details, but have in common a relatively adjusted large input $\Delta_{\mathbb{P}}$ and a diminishing $\alpha'_{\mathbb{P}}$.

Recall that, traditionally, $\Delta_{\mathbb{P}}$ determines the energy dependence of the total, elastic and diffractive cross sections while $\alpha'_{\mathbb{P}}$ determines the forward slopes. This picture is modified in updated \mathbb{P} models in which s and t unitarity screenings induce a much smaller \mathbb{P} intercept at $t=0$, denoted $\Delta_{\mathbb{P}}^{eff}$, which gets smaller with energy. The exceedingly small fitted $\alpha'_{\mathbb{P}}$ implies a partonic description of the \mathbb{P} which leads to a pQCD interpretation.

Gribov's partonic Regge theory provides the microscopic sub structure of the \mathbb{P} where the slope of the \mathbb{P} trajectory is related to the mean transverse momentum of the partonic dipoles constructing the Pomeron.

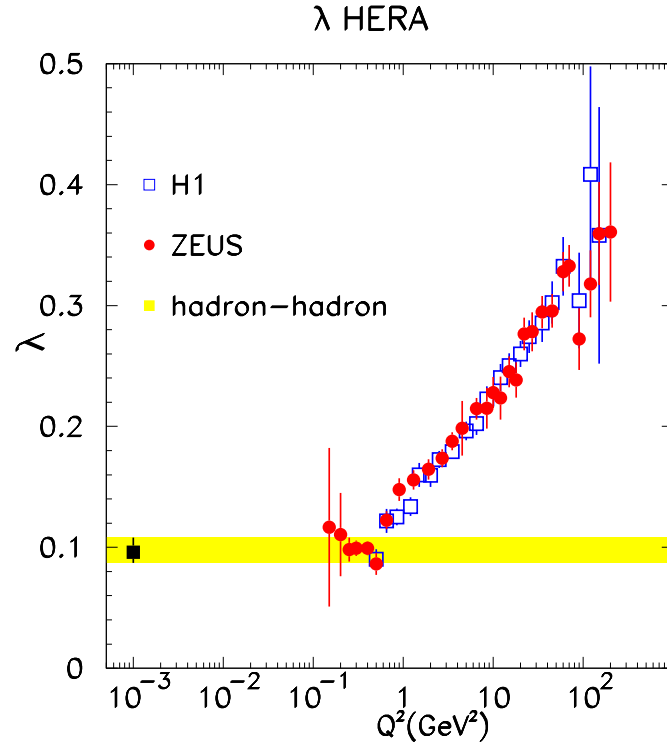
$$\alpha'_{\mathbb{P}} \propto 1 / \langle p_t \rangle^2, \quad \text{accordingly} \quad \alpha_S \propto \pi / \ln \left(\langle p_t^2 \rangle / \Lambda_{QCD}^2 \right) \ll 1.$$

We obtain a \mathbb{P} with hardness changing continuously from hard (BFKL like) to soft (Regge like). This is a non trivial relation as the soft \mathbb{P} is a simple moving pole in J-plane, while, the BFKL hard \mathbb{P} is a branch cut, approximated though, as a simple pole with $\Delta_{\mathbb{P}} = 0.2 - 0.3$, $\alpha'_{\mathbb{P}} \simeq 0$.

GLM and KMR models are rooted in Gribov's partonic \mathbb{P} theory with a hard pQCD \mathbb{P} input. It is softened by unitarity screening (GLM), or the decrease of its partons' transverse momentum (KMR). The two definitions are correlated.

GLM and KMR have a bound of validity, at 60(GLM) and 100(KMR) TeV, implied by their approximations. Consequently, as attractive as updated \mathbb{P} models are, we can not utilize them above 100 TeV.

To this end, the only relevant models are single channel, most of which have a logarithmic parametrization input. As noted, the main deficiency of these models is that they ignore the diffractive channels and their handling of unitarity screening is partial at best.



The single IP picture suggested by the updated IP models implies a smooth transition from the input hard IP to a soft IP . This picture is supported by the the HERA dependence of $\lambda = \Delta_{IP}$ on Q^2 shown in the figure above.

Note though, that a smooth transition from a soft to hard IP can be reproduced also by a 2 IP s (soft and hard) model such as Ostapchenco's.

UNITARITY SATURATION

As we saw, unitarity saturation is coupled to 2 experimental signatures:

$$\frac{\sigma_{inel}}{\sigma_{tot}} = \frac{\sigma_{el}}{\sigma_{tot}} = \mathbf{0.5},$$

$$\sigma_{diff} = \mathbf{0}.$$

Checking the experimental cross section data at the TeV-scale, we get:

- $\sigma_{inel}/\sigma_{tot} = 0.754(\text{CDF}), 0.748(\text{TOTEM}), 0.69(\text{AUGER})$.

The numbers above suggest a very slow approach toward saturation.

- **Block and Halzen single channel model, reproduces well the elastic and total cross sections, can be applied at arbitrary high energies.**

The prediction of BH at the Planck-scale ($1.22 \cdot 10^{16} \text{TeV}$) is:

$$\sigma_{inel}/\sigma_{tot} = 1131\text{mb}/2067\text{mb} = \mathbf{0.55}.$$

- **The above cross section data, supported by model predictions, implies that saturation will be attained, if at all, at non realistic energies.**

- The predicted vanishing of the diffractive cross sections at saturation implies that σ_{sd} , which up to the TEVATRON grows with energy slowly, compatible with unitarity screenings, will eventually start to reduce. This may serve as a signature that the elastic amplitude is approaching saturation.
- The preliminary TOTEM measurements suggest a severe change in the energy dependence of σ_{sd} , which is considerably smaller than its value at CDF.

$$\sigma_{sd}/\sigma_{tot} = 0.114(\text{CDF}), 0.066(\text{TOTEM}).$$

The diffractive data suggests a much faster approach toward unitarity saturation than the elastic/total data. As it stands TOTEM diffractive data is very preliminary. Never the less, the compatibility between the information derived from different channels of soft scattering deserves a very careful study!